Accepted Manuscript

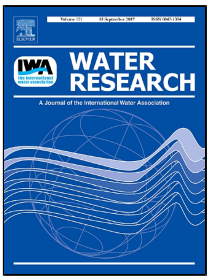

Activation of sodium persulfate by magnetic carbon xerogels (CX/CoFe) for the oxidation of bisphenol A: Process variables effects, matrix effects and reaction pathways

Alexandra Outsiou, Zacharias Frontistis, Rui S. Ribeiro, Maria Antonopoulou, Ioannis K. Konstantinou, Adrián Silva, Joaquim L. Faria, Helder T. Gomes, Dionissios Mantzavinos

PII:	S0043-1354(17)30619-X
DOI:	10.1016/j.watres.2017.07.046
Reference:	WR 13089
To appear in:	*Water Research*
Received Date:	23 May 2017
Revised Date:	17 July 2017
Accepted Date:	18 July 2017

Please cite this article as: Alexandra Outsiou, Zacharias Frontistis, Rui S. Ribeiro, Maria Antonopoulou, Ioannis K. Konstantinou, Adrián Silva, Joaquim L. Faria, Helder T. Gomes, Dionissios Mantzavinos, Activation of sodium persulfate by magnetic carbon xerogels (CX/CoFe) for the oxidation of bisphenol A: Process variables effects, matrix effects and reaction pathways, *Water Research* (2017), doi: 10.1016/j.watres.2017.07.046

Activation of sodium persulfate by magnetic carbon xerogels (CX/CoFe) for the oxidation of bisphenol A: Process variables effects, matrix effects and reaction pathways

Alexandra Outsiou[a], Zacharias Frontistis[a], Rui S. Ribeiro[b,c], Maria Antonopoulou[d], Ioannis K. Konstantinou[e], Adrián M.T. Silva[c], Joaquim L. Faria[c], Helder T. Gomes[b], Dionissios Mantzavinos[a]*

[a] *Department of Chemical Engineering, University of Patras, Caratheodory 1, University Campus,GR-26504 Patras, Greece.*

[b] *Laboratory of Separation and Reaction Engineering - Laboratory of Catalysis and Materials (LSRE-LCM), Escola Superior de Tecnologia e Gestão, Instituto Politécnico de Bragança, Campus de Santa Apolónia, 5300-253 Bragança, Portugal.*

[c] *Laboratory of Separation and Reaction Engineering – Laboratory of Catalysis and Materials (LSRE-LCM), Faculdade de Engenharia, Universidade do Porto, Rua Dr. Roberto Frias, 4200-465 Porto, Portugal.*

[d] *Department of Environmental and Natural Resources Management, University of Patras, 2 Seferi St., GR-30100 Agrinio, Greece.*

[e] *Department of Chemistry, Laboratory of Industrial Chemistry, University of Ioannina, GR-45110 Ioannina, Greece.*

*Corresponding author

E-mail: mantzavinos@chemeng.upatras.gr; Tel.: +302610996136; Fax: +302610969532

Abstract

An advanced oxidation process comprising sodium persulfate (SPS) and a novel magnetic carbon xerogel was tested for the degradation of bisphenol A (BPA), a model endocrine-disrupting compound. The catalyst, consisting of interconnected carbon microspheres with

embedded iron and cobalt microparticles, was capable of activating persulfate to form sulfate and hydroxyl radicals at ambient conditions.

The pseudo-first order degradation rate of BPA in ultrapure water (UPW) was found to increase with (i) increasing catalyst (25-75 mg/L) and SPS (31-250 mg/L) concentrations, (ii) decreasing BPA concentration (285-14200 μg/L), and (iii) changing pH from alkaline to acidic values (9 to 3).

Besides UPW, tests were conducted in drinking water, treated wastewater, groundwater and surface water; interestingly, the rate in UPW was always lower than in any other matrix containing several organic and inorganic constituents. The effect of natural organic matter (in the form of humic acids) and alcohols was detrimental to BPA degradation owing to the scavenging of radicals. Conversely, chlorides at concentrations greater than 50 mg/L had a positive effect due to the formation and subsequent participation of chlorine-containing radicals.

Liquid chromatography time-of-flight mass spectrometry was employed to identify major transformation by-products (TBPs) of BPA degradation in the absence and presence of chlorides; in the latter case, several chlorinated TBPs were detected confirming the role of Cl-related radicals. Based on TBPs, main reaction pathways are proposed.

Keywords: chloride; endocrine disruptors; Fenton-like; intermediates; operating parameters; radicals.

1. Introduction

In recent years, the use of persulfate as a source of reactive sulfate radicals (equation 1) has been considered an efficient advanced oxidation process (AOP) for water and wastewater treatment (Matzek and Carter, 2016):

$S_2O_8^{2-}$ + Activator → [$SO_4^{-\bullet}$ or SO_4^{2-}] (1)

Persulfate exhibits several advantages due to its moderate cost, high stability and aqueous solubility, as well as to the fact that it is solid at ambient temperature, which facilitates its transport and storage (Lin et al., 2011). Nonetheless, persulfate itself is a moderate oxidizing agent (E^o=2.01 V) and it must be activated to generate sulfate radicals (E^o=2.5-3.1 V), which typically react 103-105 times faster than the anion persulfate (Tsitonaki et al., 2010). Persulfate activation can be achieved by several means including heat, UV light, ultrasound, microwaves and through one-electron transfer using metals such as iron, cobalt, copper, zinc and manganese (Matzek and Carter, 2016). Persulfate activation by transition metals and, ferrous ion in particular, has extensively been investigated mimicking classical Fenton reactions (Liu et al., 2014) (equations 2-4):

$S_2O_8^{2-} + Fe^{2+} \rightarrow SO_4^{\bullet-} + SO_4^{2-} + Fe^{3+}$ (2)

$Fe^{3+} + S_2O_8^{2-} \rightarrow Fe^{2+} + S_2O_8^{\bullet-}$ (3)

Thus, the overall metal-catalyzed decomposition of persulfate can be described as follows:

$2S_2O_8^{2-} \xrightarrow{Fe(II)\leftrightarrow Fe(III)} SO_4^{\bullet-} + SO_4^{2-} + S_2O_8^{\bullet-}$ (4)

In Fenton and alike systems, the use of homogeneous iron (or other ions) typically requires an additional step for the recovery and/or elimination of metals from the treated stream prior to final discharge. Several attempts have been made to overcome this drawback through immobilization of the active phase on a suitable support, i.e. activated carbon, alumina, silica, mesoporous molecular sieves, zeolites, pillared clays and ion-exchange resins (Nidheesh, 2015). Nevertheless, this approach may result in reduced efficiency associated with decreased catalyst stability and/or increased mass transfer limitations (Ribeiro et al., 2016a).

A set of novel magnetic carbon xerogels, consisting of interconnected carbon microspheres with iron and/or cobalt microparticles embedded in their structure, has recently been prepared by inclusion of iron and/or cobalt precursors during the synthesis of carbon xerogels by polycondensation of resorcinol with formaldehyde, followed by thermal annealing at 800°C.

The catalysts have extensively been characterized and tested successfully for the oxidation of the antibiotic sulfamethoxazole in water using hydrogen peroxide as the source of hydroxyl radicals; these materials exhibited high activity and good stability and they were also magnetically recoverable post-treatment (Ribeiro et al., 2016b).

The work reported in this paper deals for the first time with the use of magnetic carbon xerogels as possible activators of persulfate to oxidize bisphenol A (BPA) in various aqueous matrices. BPA is an emerging micro-contaminant belonging to the family of endocrine disruptors and it has been chosen as a model compound due its excessive usage in plastics manufacturing, as well as additive in brake fluids, thermal papers and flame retardants (Oehlmann et al., 2008). BPA exhibits weak estrogenic activity at concentrations as low as few ng/L-μg/L, while it is resistant to biodegradation (Vandenberg et al., 2007). It can be released in the environment through various paths including municipal wastewater treatment plant discharges, landfill leachates and spillovers during storage/transportation (Huang et al., 2012).

The goal of this work was to study the effect of various operating parameters such as the concentration of catalyst, the concentration of persulfate, the concentration of BPA and the solution pH on the kinetics of degradation. Particular emphasis was given on the effect of the matrix complexity testing several environmentally relevant water matrices. In addition, major transformation by-products were identified and possible reaction pathways and mechanisms were proposed, taking into consideration the interferences of the water matrix constituents.

2. Materials and methods

2.1 Magnetic carbon xerogels

Experiments were performed with a bimetallic carbon xerogel consisting of interconnected carbon microspheres with iron and cobalt microparticles embedded in their structure

(CX/CoFe). Cobalt ferrite ($CoFe_2O_4$) is the dominant phase. The procedures for catalyst synthesis and characterization are described in detail elsewhere (Ribeiro et al., 2016b).

2.2 Chemicals

Bisphenol A (BPA, $C_{15}H_{16}O_2$, CAS number: 80-05-7) and sodium persulfate (SPS, $Na_2S_2O_8$, 99+%, CAS number: 7775-27-1) were purchased from Merck.

Humic acid (technical grade), hydrogen peroxide (30%), sodium chloride (99.8%), sodium hydroxide (98%), boric acid (>99.8%) and sulphuric acid (95%) were also obtained from Merck. Methanol (99.9%) and t-butanol (99%) were purchased from Fluka, while potassium dihydrogen phosphate from Millipore.

All chemicals were used as received, without further purification.

2.3 Water matrices

BPA solutions were prepared in (i) ultrapure water (UPW); (ii) secondary treated wastewater (WW) collected from the wastewater treatment plant of the University of Patras campus, Greece; (iii) drinking water (DW) obtained from a bottle of the commercially available brand Avra®, Greece; (iv) surface water taken from a rivulet in the region of Athens, Greece; (v) groundwater taken from a borehole in the region of Athens, Greece. Properties of the various matrices are summarized in Table 1.

2.4 Experimental procedure

In a typical experiment, 120 mL of an aqueous solution containing the desired concentration of BPA was loaded in a glass cylindrical reaction vessel. The appropriate amount of SPS and the catalyst were then added and the reaction took place under magnetic stirring in open air equilibrium. Unless otherwise stated, the solution was buffered at acidic, near-neutral or

alkaline conditions using the appropriate buffers (see section 3.1). Samples of 1.2 mL were periodically withdrawn from the reactor, quenched with methanol, filtered to remove any solid particles and analyzed by chromatography.

Most of the experiments were performed in duplicate and mean values (<5% difference) are quoted as results.

2.5 Analytical methods

High performance liquid chromatography was employed to monitor the concentration of BPA. The analytical protocol (columns, mobile phase, detector) is described in detail elsewhere (Darsinou et al., 2015). The limit of detection was 4.7 μg/L and the limit of quantitation was 12.4 μg/L.

Liquid chromatography time-of-flight mass spectrometry (LC-TOF-MS) operated in negative ionization mode was used for the identification of transformation by-products (TBPs) as described in detail in our previous work (Darsinou et al., 2015). LC analyses were run with water (LC-MS grade) with 0.01% formic acid (solvent A) and acetonitrile (solvent B) as mobile phase with a flow rate of 0.3 mL/min. A linear gradient was run as follows: 1% B (initial conditions) to 99% B in 15 min and then returned to 1% B after 3 min.

3. Results and discussion

3.1 Effect of solution pH

The effect of solution pH on BPA degradation was studied at three values, i.e. 3, 6 and 9. The results are shown in Figure 1. Near-neutral and alkaline conditions were achieved using KH_2PO_4 and a mixture of NaOH and H_3BO_3 as buffers, respectively, while acidic conditions were achieved adding H_2SO_4, which also served as buffer; in all cases, the pH remained unchanged during the reaction. Although complete BPA degradation can be achieved within

45-60 min regardless of the starting solution pH, the initial rate decreases with increasing pH. The point of zero charge of the catalyst is 7.7 (Ribeiro et al., 2016b), therefore, it is positively charged at pH<7.7. Consequently, the adsorption and subsequent activation of persulfate anions onto the catalysts is favored at pH values of 3 and 6 due to the electrostatic attraction between the catalyst surface and the persulfate ions but it decreases at pH=9 due to electrostatic repulsion. In addition, the presence of insoluble forms of Fe(II)/Fe(III) under neutral and alkaline pH could be also considered for the slower kinetics obtained at pH 6 and 9.

Furthermore, BPA whose pKa is 9.6-10.2 (Bautista-Toledo et al., 2005), is negatively charged at alkaline pH range above the pKa value, therefore, an electrostatic repulsion between the substrate and the catalyst cannot be considered to affect significantly the degradation kinetics and thus the decreased reactivity recorded at pH=9.

Finally, sulfate radicals react with water at all pH values leading to the formation of hydroxyl radicals, which become the main oxidizing species at alkaline conditions (Matzek and Carter, 2016; Zhao et al., 2014), according to equations 5 and 6:

$SO_4^{\bullet-} + H_2O \rightarrow SO_4^{2-} + {}^{\bullet}OH + H^+$ (5)

$SO_4^{\bullet-} + OH^- \rightarrow SO_4^{2-} + {}^{\bullet}OH$ (6)

Although sulfate radicals have a lower redox potential than hydroxyl radicals, they are more selective towards certain organics (Darsinou et al., 2015; Lutze et al., 2015) and this may justify the reactivity recorded at lower pH values, where sulfate radicals prevail.

Additional experiments (not shown for brevity) were performed adjusting but not buffering the initial solution pH from its inherent value of 6 to 9 (with NaOH) or 3 (with H_2SO_4). For the run at pH_o=6, the value rapidly dropped to 4.3 within the first 2 min of reaction and eventually stabilized to 4±0.2 for the rest of the reaction; at these conditions, the BPA degradation profile nearly matched that at pH_o=3. For the run at pH_o=9, the degradation was

177 always 15-20% lower than at the other two pHs, with pH dropping and stabilizing at near-
178 neutral values.

179 These results indicate that the proposed treatment system can function efficiently in a wide
180 range of pH values, which makes its application feasible for water/wastewater treatment
181 without the need for pH buffering or adjustment (i.e. at the sample's natural pH). However
182 and for the purposes of this study, all subsequent experiments were performed at pH=3 in
183 order to eliminate the effect of pH change during the reaction.

184

185 *3.2 Effect of catalyst and SPS concentration*

186 Based on the knowledge for Fenton and Fenton-like reactions in which the concentration
187 levels of the catalyst and the oxidant are crucial to process performance, the effect of these
188 parameters are also studied herein. Figure 2 shows the beneficial effect of increasing catalyst
189 concentration in the range 25-75 mg/L on the degradation of 285 μg/L BPA. Considering that
190 BPA concentration-time profiles can be fitted adequately (i.e. the linear regression coefficient,
191 r^2, is >95%) to a pseudo-first order rate expression (equation 7):

192 $$\ln\frac{C_o}{C} = k_{app}t \Leftrightarrow \ln(1-X) = -k_{app}t \quad (7)$$

193 the apparent rate constant for BPA degradation, k_{app}, is computed equal to 0.013, 0.038 and
194 0.094 min^{-1} at 25, 50 and 75 mg/L catalyst concentration, respectively. In the absence of
195 catalyst, SPS cannot be activated to form radicals and this is consistent with the low extent
196 (*ca* 10%) of BPA degradation recorded (this is due to the fact that SPS itself is a mild
197 oxidant).

198 Figure 3 shows the effect of changing SPS concentration in the range 31-500 mg/L on the
199 degradation of 285 μg/L BPA. The computed k_{app} values according to equation 7 are 0.054,
200 0.069, 0.086, 0.093 and 0.046 min^{-1} at 31, 62.5, 125, 250 and 500 mg/L SPS, respectively (the
201 linear regression coefficient, r^2, is >97%). Degradation increases with increasing SPS

concentration up to a point, beyond which the effect becomes detrimental; it is well-documented (Dewil et al., 2017) that an excess of oxidant in Fenton and alike systems may result in radical self-scavenging effects, thus decreasing performance. From the experiment without SPS, it is evident that BPA is partly adsorbed onto the catalyst surface (i.e. 30% after 45 min, which is extended to 35% after 90 min (not shown in Figure 3)).

We have recently demonstrated (Ribeiro et al., 2016b) that carbon xerogels are effective heterogeneous Fenton catalysts for the degradation of antibiotics in various matrices. In this light, an additional experiment was performed replacing SPS with an equal concentration of H_2O_2; as can be seen in Figure 3, the reaction with 250 mg/L H_2O_2 is substantially slower leading to only 63% BPA degradation after 45 min.

3.3 Effect of BPA concentration

Although the pseudo-first order approach is useful to depict apparent rate constants and, consequently, quantify kinetics, this does not necessarily imply that the reaction is indeed true first order with respect to the substrate. This is clearly demonstrated in Figure 4 where the time needed to achieve a certain BPA conversion, X (see also equation 7), depends on its initial concentration. For example, the time needed to achieve 85% BPA conversion is 15, 45 and 120 min at 285, 570 and 855 μg/L BPA concentration, respectively; moreover, the corresponding k_{app} are also concentration-dependent taking values of 0.093, 0.042 and 0.019 min^{-1} (r^2 is >94%). As the amount of generated oxidizing species available to react with the substrate mainly depends on the operating conditions (i.e. catalyst and SPS concentration, pH), kinetics will predominantly be dictated by the substrate concentration; as the latter increases, the reaction order will shift to lower values and, eventually, become zero.

Although a proper kinetic analysis is outside the scope of this work, the authors would like to emphasize a common misconception made by several researchers in the field concerning the difference between (i) apparent and true rate orders, and (ii) kinetic modeling and data fitting.

In several cases, such mistakes are triggered by the unrealistically high contaminant concentrations, e.g. in the order of mg/L, employed in advanced oxidation studies. Figure 4 also shows an experiment at 14.2 mg/L BPA concentration leading to just 30% degradation after 120 min. The run was repeated doubling the SPS (500 mg/L) and catalyst (150 mg/L) concentrations and extended to 420 min after which BPA degradation was just 50% (run not shown for brevity).

3.4 The water matrix effect

The majority of published research on AOPs for water remediation is being performed in model aqueous solutions containing the contaminant under consideration. Most commonly, the contaminant is spiked in ultrapure water (UPW) at concentrations that typically are several orders of magnitude greater than those found in actual environmental samples (see section 3.3). This approach has certain advantages since (i) it eliminates the interactions amongst the contaminant, the oxidative species and the constituents of more complex matrices (i.e. surface water, groundwater, municipal wastewater), (ii) it does not require sophisticated and laborious analytical techniques to monitor trace amounts of the contaminant.

The quality of the actual water matrix is critical since not taking into account the various interactions is likely to lead to false conclusions. As a rule of thumb, degradation kinetics decrease with increasing matrix complexity mainly because the matrix may contain several non-target organic and inorganic constituents that compete with the target molecule(s) for the oxidizing species.

Figure 5 shows BPA degradation in various water matrices such as UPW, drinking water (DW), surface water taken from a rivulet, groundwater and secondary treated wastewater (WW). Although complete BPA degradation can be achieved within 30-45 min of reaction irrespective of the matrix employed, the initial rate clearly depends on it. Interestingly, and

unlikely to what was expected, the reaction in UPW is slower than in any other matrix including WW, which contains, besides various inorganic anions, organic carbon in the order of 10 mg/L.

Humic acids and low molecular weight organic acids such as oxalate are able to form complexes with iron and iron oxides, thus promoting the Fenton-like oxidation processes. On the contrary, the presence of organic matter and inorganic anions could result in competitive adsorption in relation to persulfate anions and substrate onto the xerogel surface, as well as in scavenging of the produced radicals. The observed kinetics is the overall result of interplay among the previous effects and thus we attempted to discriminate the role of the major constituents.

3.4.1 The role of organic constituents

To check the effect of the organic matter, experiments were conducted adding humic acid (HA) in UPW, a representative of the organic matter typically found in natural waters and wastewaters and the results are shown in Figure 6. The apparent rate constant of BPA degradation in UPW is 0.093 min^{-1} and it decreases to 0.058 and 0.036 min^{-1} in the presence of 5 and 20 mg/L HA, respectively. It should be noted here that the organic carbon content of 20 mg/L HA is nearly equal to that found in WW. Additional experiments were performed with methanol and t-butanol, which are typical radical scavengers showing different affinity to hydroxyl and sulfate radicals; methanol reacts with the former 300 times faster than with the latter, while t-butanol 1900 times faster (Qi, et al., 2015). The presence of both alcohols retards BPA degradation (the rate constants are 0.031 and 0.023 min^{-1} with methanol and t-butanol, respectively), indicating that both sulfate and hydroxyl radicals are responsible for BPA degradation. From the results of Figures 5 and 6, it is inferred that the beneficial water matrix effect on BPA degradation cannot be ascribed to the presence of non-target organic constituents as these appear to compete directly with BPA for the oxidizing species. This is

also consistent with the effect of initial BPA concentration on its degradation, particularly at excessive concentrations as depicted in Figure 4.

3.4.2 The role of chloride ion

Various ions naturally occurring in water matrices may affect the performance of activated persulfate oxidation with bicarbonate and chloride ions playing an important role. The way these ions interfere with the process is case-specific depending on the persulfate activation method, the type of substrate, the complexity of the water matrix and the concentration levels of the ions under consideration; in this respect, it is not surprising that various studies have reported both detrimental and beneficial effects of ions on substrate degradation (Matzek and Carter, 2016; Lutze et al., 2015; Bennedsen et al., 2012; Fang et al., 2012).

The effect of chloride in the range 50-500 mg/L on BPA degradation over the CX/CoFe catalyst is shown in Figure 7. The reaction rate increases by as much as six times when the solution is added 200 mg/L chloride, while a higher concentration of 500 mg/L does not accelerate the reaction further. Blank experiments were also performed (not shown for brevity) with NaCl alone (i.e. without catalyst and SPS) and NaCl and SPS (i.e. without catalyst) yielding no BPA degradation.

Sulfate radicals primarily react with chloride to form chlorine radicals (equation 8) that further react with chloride to form the dichloride radical (equation 9) (Lutze et al., 2015; Bennedsen et al., 2012; Fang et al., 2012):

$SO_4^{\bullet-} + Cl^- \rightleftarrows SO_4^{2-} + Cl^{\bullet}$ (8)

$Cl^{\bullet} + Cl^- \rightleftarrows Cl_2^{\bullet-}$ (9)

Depending on the experimental conditions under consideration, several consecutive reactions may take place leading to the formation of additional chlorine-containing radicals such as $ClO_2^{\bullet}$, $ClO^{\bullet}$ and $HOCl^{\bullet-}$ (Lutze et al., 2015). From these results, one can safely assume that

the presence of chloride influences the distribution and relative concentration of reactive radicals, consequently altering the reactivity towards BPA degradation. Similarly to the present results, the degradation of phenol and 2,4-dichlorophenol by cobalt-activated peroxymonosulfate was promoted in the presence of chloride (Anipstitakis et al., 2006). In addition, chlorine radicals can influence the catalytic step of Fe(II)/Fe(III) conversion, thus regenerating iron in its initial state of Fe(III) in the cobalt ferrite spinel:

$Fe^{2+} + Cl^{\bullet} \rightarrow Fe^{3+} + Cl^{-}$ (10)

$Fe^{2+} + Cl_2^{\bullet-} \rightarrow Fe^{3+} + 2Cl^{-}$ (11)

At acidic conditions (pH<4), the equilibrium between the bicarbonate ion and CO_2 is completely shifted towards the latter and, in this respect, one might have expected no effect of bicarbonate on the process at the working pH value of 3. Interestingly, experiments with 500 mg/L of bicarbonate (data not shown for brevity) resulted in ca 50% reduction of BPA degradation rate (i.e. from 0.093 to 0.045 min^{-1}). As the solution was not purged prior to the experiment to accelerate the release of CO_2 in the atmosphere, the bicarbonate ion may still be present in the solution; its detrimental effect on degradation is associated with the scavenging of both sulfate and hydroxyl radicals to form carbonate radicals (Vicente et al., 2011).

3.5. Mechanisms and pathways of degradation

To shed light to the mechanisms of BPA degradation in the presence and absence of chloride, samples were subject to LC-TOF-MS analysis to identify transformation by-products (TBPs). The respective data are summarized in Table 2. A total number of 11 and 15 TBPs were identified in the absence and presence of NaCl, respectively. According to these results, polymerization pathways through radicals coupling were followed in the initial steps of degradation both in the absence and presence of NaCl. The structures of BPA oligomers (dimers, trimers and tetramers), as well as their formation pathways are depicted in Figure 8.

In general, for phenolic compounds, the formation of oligomers proceeds through C-C coupling and/or C-O coupling. Among the two routes, C-C coupling (ortho-para and ortho-ortho links) is a more favorable route, which is energetically promoted (Ežerskis and Jusys, 2001). However, it should be pointed out that TBPs with etheric structures have also been identified previously via C-O coupling of phenoxyl radicals and their formation can also be expected (Ežerskis and Jusys, 2001).

Alongside the formation of dimers, trimers and tetramers, three other coupling TBPs (TBP2, TBP4, TBP5) have been identified both in the absence and presence of NaCl. Their formation pathways is depicted in Figure 9 and can be rationalized through the bimolecular coupling of BPA radicals (I) and other radicals (e.g. V, VI, VII) originated from hydrogen abstraction and β-scission of BPA and hydroxy-BPA.

Similar TBPs with oligomeric structures, as well as TBPs formed by coupling of different radicals generated during the process have also been identified during the oxidation of BPA by heat-activated persulfate (Potakis et al., 2017).

Besides the similarities in degradation pathways, some major differences are also pointed out. In the presence of NaCl, chloro- and dichloro-BPA (TBP6 and TBP7) are formed at the first stages of the reaction (Figure 10). Chlorine-substituted BPA derivatives have also been reported in the literature during the chlorination of BPA molecule through a chlorine-substitution reaction on the aromatic ring, followed by dehydration as the proposed mechanism (Gallard et al., 2004; Hu et al., 2002). Based on literature data (Gallard et al., 2004; Hu et al., 2002), 2-chloro-BPA, 2,6'-dichloro-BPA or 2,6-dichloro-BPA can be postulated.

The rapid formation of chloro- and dichloro-BPA in combination with the high abundance of their peaks justifies the fast kinetics of BPA degradation observed in the presence of NaCl. The formation of TBP6 and TBP7 is followed by various chlorinated dimers and trimers, as a result of coupling reactions depicted in Figure 10. However, in the absence of NaCl, the

356 degradation of BPA also proceeds through hydroxylation and oxidation reactions (Potakis et
357 al., 2017; Sharma et al., 2016) that can occur in the aromatic ring and isopropyl group (Figure
358 11). These pathways were not observed in the presence of NaCl within the same time
359 framework of treatment.
360 Although the concentration profiles of TBPs were not possible to be followed due to their fast
361 formation and dissipation, taking into account their relative abundance, it can be proposed
362 that radical coupling reactions are the main transformation pathways during the first stages of
363 the treatment, both in the presence and absence of NaCl. Comparing the polymerization
364 routes in the presence of NaCl, the formation of chlorinated dimers and trimers is
365 undoubtedly favored, proving the major role of chlorine radicals ($Cl^{\bullet}$) formed through the
366 direct reaction of Cl^- with $SO_4^{\bullet-}$ radicals, as also evidenced elsewhere (Lutze et al., 2015).
367

368 4. Conclusions
369 The primary conclusions derived from this study are as follows:
370 1) The rate of BPA degradation is a function of the operating variables, including catalyst,
371 oxidant and substrate concentrations, solution pH and treatment time. Similarly to other
372 Fenton-like AOPs, the rate increases with increasing catalyst and oxidant concentrations,
373 although excessive levels may introduce radical scavenging effects. Furthermore, the rate
374 decreases with increasing substrate concentration, which highlights the need to perform
375 studies with environmentally reasonable concentrations.
376 2) Unlike what typically happens in the advanced oxidation of various organics, BPA
377 degradation in environmentally relevant matrices is faster than in pure water; this pinpoints
378 the rather complicated interferences amongst the various organic and inorganic constituents
379 found in actual water matrices.
380 3) The individual effects of humic acid, alcohols, bicarbonate and chloride ions were

appraised; organics and the bicarbonate ion act as scavengers of sulfate and hydroxyl radicals, thus leading to reduced degradation, while chlorides act as a source of extra Cl-containing radicals, thus leading to increased degradation.

4) BPA degradation is accompanied by the formation of several TBPs and occurs through (i) polymerization reactions, (ii) bimolecular coupling between BPA-radicals and other radicals, and (iii) hydroxylation/oxidation reactions. Reactions in the presence of chlorides lead to the formation of chlorinated TBPs.

Acknowledgments

Z. Frontistis would like to thank the Greek State Scholarships Foundation (IKY) for the financial support of this research through the "IKY Fellowships of Excellence for Postgraduate Studies in Greece – Siemens Programme" in the framework of the Hellenic Republic – Siemens Settlement Agreement.

Part of this work was financially supported by: Project POCI-01-0145-FEDER-006984 - Associate Laboratory LSRE-LCM funded by FEDER through COMPETE2020 – Programa Operacional Competitividade e Internacionalização (POCI) - and by national funds through FCT - Fundação para a Ciência e a Tecnologia. R.S. Ribeiro acknowledges the FCT individual Ph.D. grant SFRH/BD/94177/2013, with financing from FCT and the European Social Fund (through POPH and QREN). A.M.T. Silva acknowledges the FCT Investigator 2013 Programme (IF/01501/2013), with financing from the European Social Fund and the Human Potential Operational Programme.

403 References

404

405 Anipsitakis, G.P., Dionysiou, D.D., Gonzalez, M.A., 2006. Cobalt-mediated activation of
406 peroxymonosulfate and sulfate radical attack on phenolic compounds. Implications of
407 chloride ions. Environmental Science & Technology 40 (3), 1000-1007.
408 Bautista-Toledo, I., Ferro-Garcia, M.A., Moreno-Castilla, C., Vegas Fernandez, F.J., 2005.
409 Bisphenol A removal from water by activated carbon. Effects of carbon characteristics and
410 solution chemistry. Environmental Science & Technology 39 (16), 6246-6250.
411 Bennedsen, L.R., Muff, J. Sogaard, E.G., 2012. Influence of chloride and carbonates on the
412 reactivity of activated persulfate. Chemosphere 86 (11), 1092-1097.
413 Darsinou, B., Frontistis, Z., Antonopoulou, M., Konstantinou, I., Mantzavinos, D., 2015.
414 Sono-activated persulfate oxidation of bisphenol A: Kinetics, pathways and the controversial
415 role of temperature. Chemical Engineering Journal 280, 623-633.
416 Dewil, R., Mantzavinos, D., Poulios, I., Rodrigo, M.A., 2017. New perspectives for advanced
417 oxidation processes. Journal of Environmental Management 195, 93-99.
418 Ežerskis, Z., Jusys, J., 2001. Electropolymerization of chlorinated phenols on a Pt electrode in
419 alkaline solution Part I: A cyclic voltammetry study. Journal of Applied Electrochemistry, 31
420 (10) 1117-1124.
421 Fang, G.D., Dionysiou, D.D., Wang, Y., Al-Abed, S.R., Zhou, D.M., 2012. Sulfate radical-
422 based degradation of polychlorinated biphenyls: Effects of chloride ion and reaction kinetics.
423 Journal of Hazardous Materials 227-228, 394-401.
424 Gallard, H., Leclercq, A., Croué, J.P., 2004. Chlorination of bisphenol A: kinetics and by-
425 products formation. Chemosphere 56 (5), 465-473.
426 Hu, J.Y, Aizawa, T., Ookubo, S., 2002. Products of aqueous chlorination of BPA and the
427 estrogenic activity. Environmental Science & Technology 36 (9), 1980-1987.

428 Huang, Y.Q., Wong, C.K.C., Zheng, J.S., Bouwman, H., Barra, R., Wahlstrom, B., Neretin,
429 L., Wong, M.H., 2012. Bisphenol A (BPA) in China: a review of sources, environmental
430 levels, and potential human health impacts. Environment International 42, 91-99.
431 Lin, Y.T., Liang, C., Chen, J.H., 2011. Feasibility study of ultraviolet activated persulfate
432 oxidation of phenol. Chemosphere 82 (8), 1168-1172.
433 Liu, H., Bruton, T.A., Doyle, F.M., Sedlak, D.L., 2014. In situ chemical oxidation of
434 contaminated groundwater by persulfate: Decomposition by Fe(III)- and Mn(IV)-containing
435 oxides and aquifer materials. Environmental Science & Technology 48 (17), 10330-10336.
436 Lutze, H.V., Kerlin, N., Schmidt, T.C., 2015. Sulfate radical-based water treatment in
437 presence of chloride: Formation of chlorate, inter-conversion of sulfate radicals into hydroxyl
438 radicals and influence of bicarbonate. Water Research 72, 349-360.
439 Matzek, L.W., Carter, K.E., 2016. Activated persulfate for organic chemical degradation: A
440 review. Chemosphere 151, 178-188.
441 Nidheesh, P.V., 2015. Heterogeneous Fenton catalysts for the abatement of organic pollutants
442 from aqueous solution: a review. RSC Advances 5, 40552-40577.
443 Oehlmann, J., Oetken, M., Schulte-Oehlmann, U., 2008. A critical evaluation of the
444 environmental risk assessment for plasticizers in the freshwater environment in Europe, with
445 special emphasis on bisphenol A and endocrine disruption. Environmental Research 108 (2),
446 140-149.
447 Potakis, N., Frontistis, Z., Antonopoulou, M., Konstantinou, I., Mantzavinos, D., 2017.
448 Oxidation of bisphenol A in water by heat-activated persulfate. Journal of Environmental
449 Management 195, 125-132.
450 Qi, C., Liu, X., Zhao, W., Lin, C., Ma, J., Shi, W., Sun, Q., Xiao, H., 2015. Degradation and
451 dechlorination of pentachlorophenol by microwave-activated persulfate. Environmental
452 Science & Pollution Research 22 (6), 4670-4679.

453 Ribeiro, R.S., Silva, A.M.T., Figueiredo, J.L., Faria, J.L., Gomes, H.T., 2016a. Catalytic wet
454 peroxide oxidation: a route towards the application of hybrid magnetic carbon
455 nanocomposites for the degradation of organic pollutants. A review. Applied Catalysis B -
456 Environmental 187, 428-460.
457 Ribeiro, R.S., Frontistis, Z., Mantzavinos, D., Venieri, D., Antonopoulou, M., Konstantinou,
458 I., Silva, A.M.T., Faria, J.L., Gomes, H.T., 2016b. Magnetic carbon xerogels for the catalytic
459 wet peroxide oxidation of sulfamethoxazole in environmentally relevant water matrices.
460 Applied Catalysis B - Environmental 199, 170-186.
461 Sharma, J., Mishra, I.M., Kumar, V., 2016. Mechanistic study of photo-oxidation of bisphenol
462 A (BPA) with hydrogen peroxide (H_2O_2) and sodium persulfate (SPS). Journal of
463 Environmental Management 166, 12-22.
464 Tsitonaki, A., Petri, B., Crimi, M., Mosbaek, H., Siegrist, R.L., Bjerg, P.L., 2010. In situ
465 chemical oxidation of contaminated soil and groundwater using persulfate: A review. Critical
466 Reviews in Environmental Science & Technology 40 (1), 55-91.
467 Vandenberg, L.N., Hauser, R., Marcus, M., Olea, N., Welshons, W.V., 2007. Human
468 exposure to bisphenol A (BPA). Reproductive Toxicology 24 (2), 139-177.
469 Vicente, F., Santos, A., Romero, A., Rodriguez, S., 2011. Kinetic study of diuron oxidation
470 and mineralization by persulphate: effects of temperature, oxidant concentration and iron
471 dosage method. Chemical Engineering Journal 170 (1), 127-135.
472 Zhao, L., Hou, H., Fujii, A., Hosomi, M., Li, F., 2014. Degradation of 1,4-dioxane in water
473 with heat- and Fe^{2+}-activated persulfate oxidation. Environmental Science & Pollution
474 Research 21 (12), 7457-7465.

Table captions

Table 1. Properties of the water matrices used in this work. ND: not determined.

Table 2. High resolution accurate mass data ($[M-H]^-$, and relative error Δ(ppm)) for BPA and TBPs (a) in the absence of NaCl, and (b) in the presence of NaCl.

Figure captions

Figure 1. Effect of buffered solution pH on 285 μg/L BPA degradation with 75 mg/L CX/CoFe and 250 mg/L SPS in UPW.

Figure 2. Effect of CX/CoFe concentration on 285 μg/L BPA degradation with 250 mg/L SPS in UPW and pH=3.

Figure 3. Effect of SPS concentration on 285 μg/L BPA degradation with 75 mg/L CX/CoFe in UPW and pH=3. Dashed line shows experiment with 250 mg/L hydrogen peroxide (HP) in otherwise identical conditions.

Figure 4. Effect of initial BPA concentration on its degradation with 75 mg/L CX/CoFe and 250 mg/L SPS in UPW and pH=3.

Figure 5. Effect of actual water matrix on 285 μg/L BPA degradation with 75 mg/L CX/CoFe, 250 mg/L SPS and pH=3.

Figure 6. Effect of organics on 285 μg/L BPA degradation with 75 mg/L CX/CoFe and 250 mg/L SPS in UPW and pH=3.

Figure 7. Effect of NaCl on 285 μg/L BPA degradation with 75 mg/L CX/CoFe and 250 mg/L SPS in UPW and pH=3.

Figure 8. BPA transformation pathways by BPA-radical coupling during treatment with CX/CoFe and SPS in the presence and absence of NaCl.

Figure 9. BPA transformation pathways by radical coupling after β-scission of BPA-radical during treatment with CX/CoFe and SPS in the presence and absence of NaCl.

500 **Figure 10.** BPA transformation pathways during treatment with CX/CoFe and SPS in the
501 presence of NaCl.

502 **Figure 11.** Hydroxylation degradation pathways of BPA during treatment with CX/CoFe and
503 SPS in the absence of NaCl.

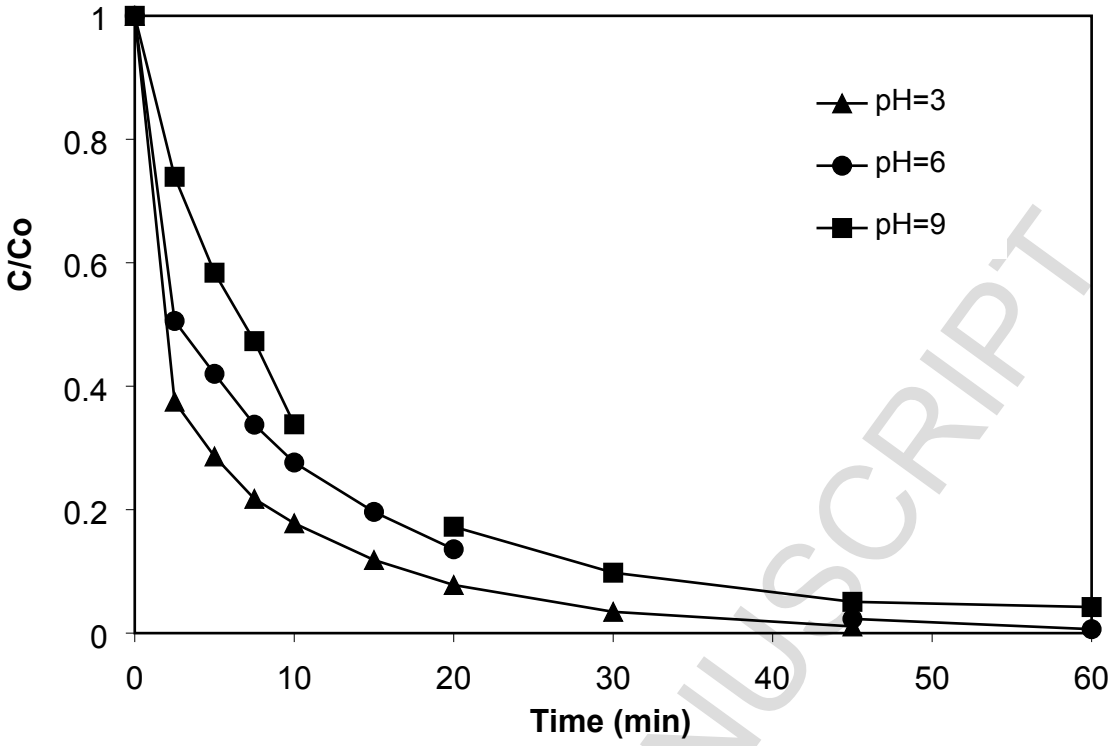

Figure 1. Effect of buffered solution pH on 285 µg/L BPA degradation with 75 mg/L CX/CoFe and 250 mg/L SPS in UPW.

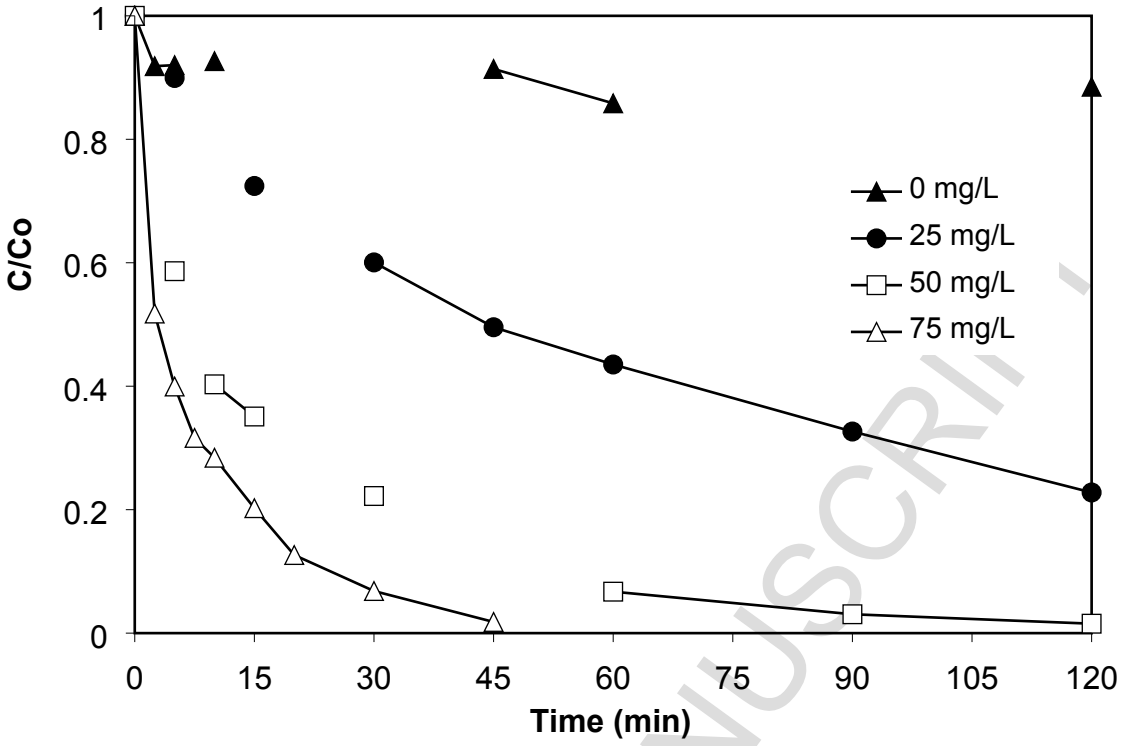

Figure 2. Effect of CX/CoFe concentration on 285 μg/L BPA degradation with 250 mg/L SPS in UPW and pH=3.

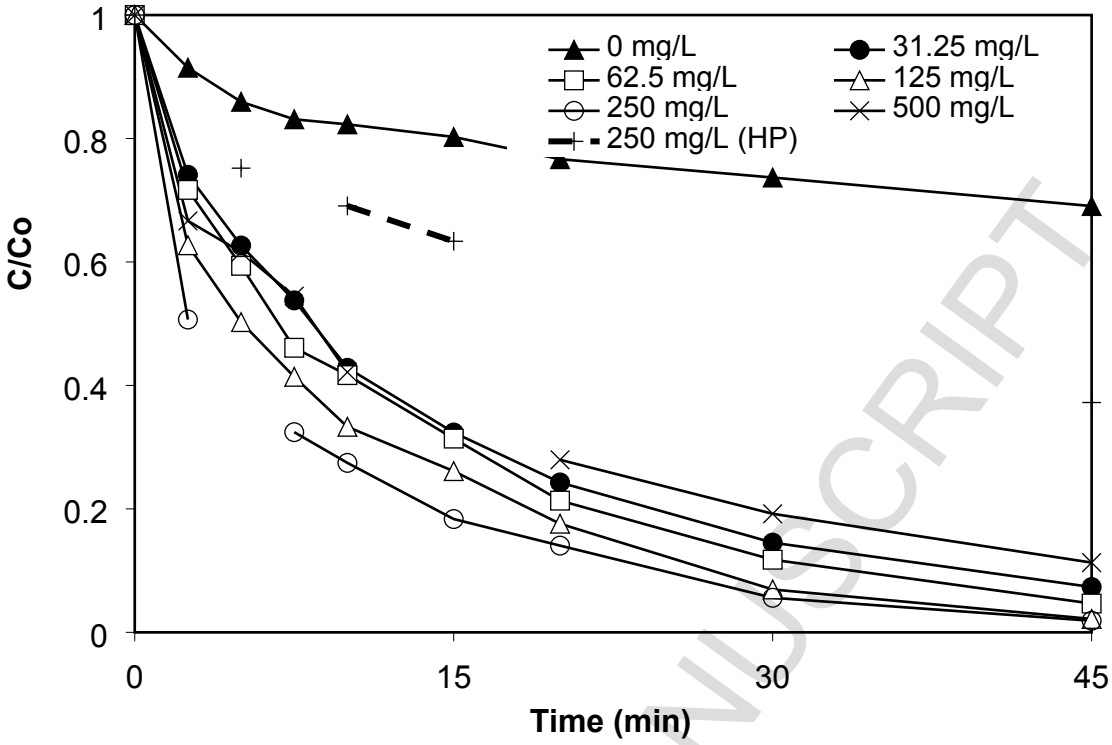

Figure 3. Effect of SPS concentration on 285 μg/L BPA degradation with 75 mg/L CX/CoFe in UPW and pH=3. Dashed line shows experiment with 250 mg/L hydrogen peroxide (HP) in otherwise identical conditions.

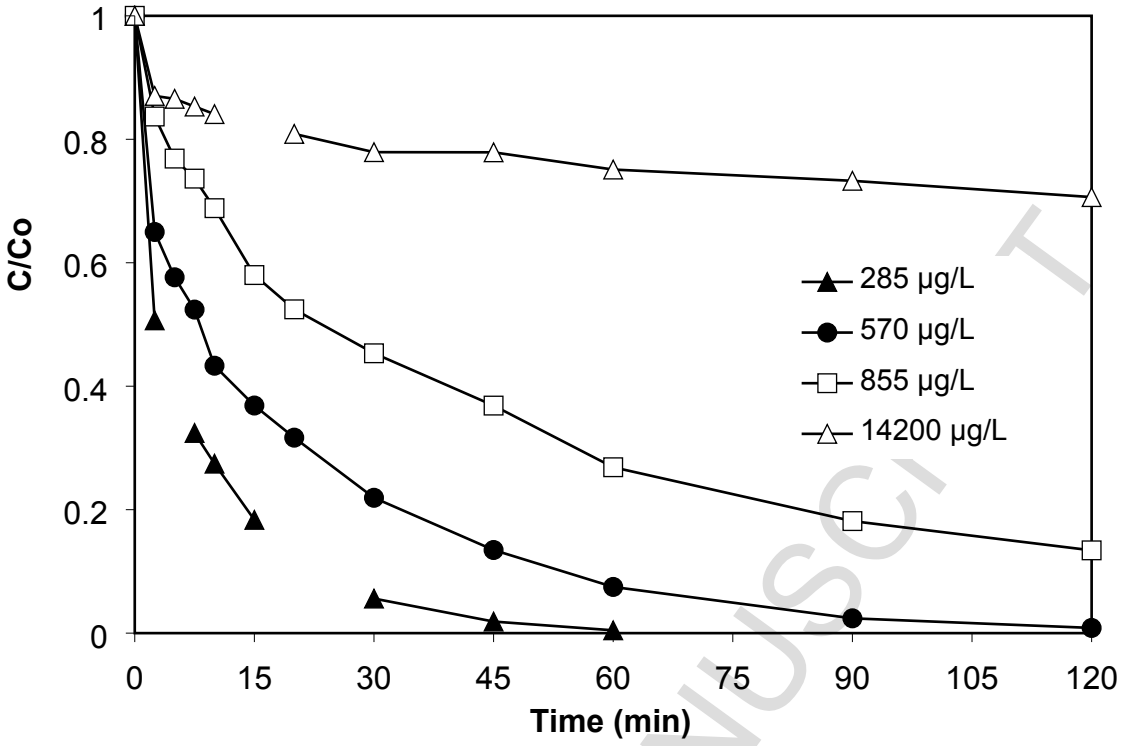

Figure 4. Effect of initial BPA concentration on its degradationwith 75 mg/L CX/CoFe and 250 mg/L SPS in UPW and pH=3.

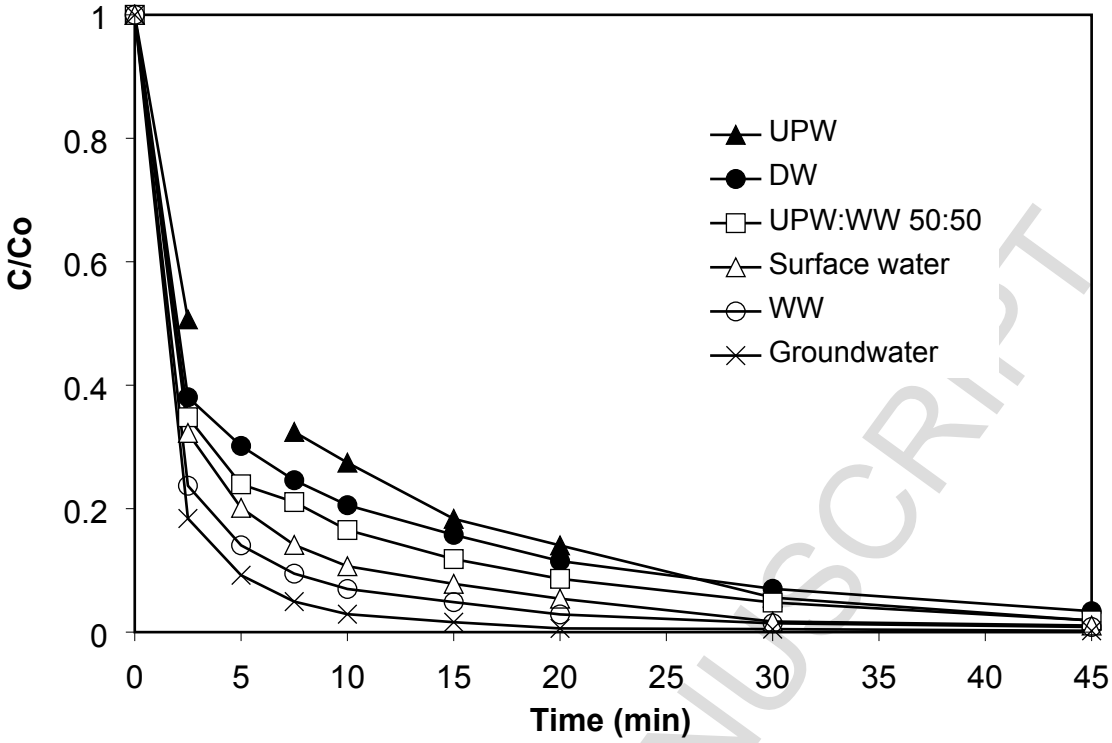

Figure 5. Effect of actual water matrix on 285 µg/L BPA degradation with 75 mg/L CX/CoFe, 250 mg/L SPS and pH=3.

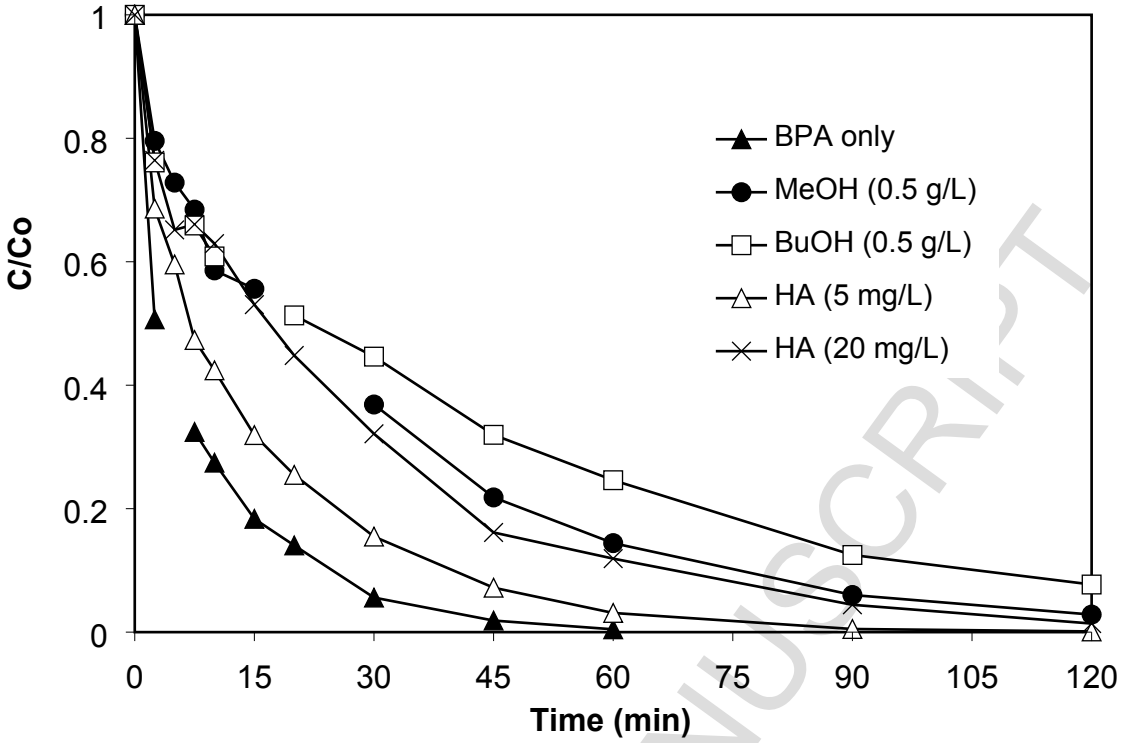

Figure 6. Effect of organics on 285 μg/L BPA degradation with 75 mg/L CX/CoFe and 250 mg/L SPS in UPW and pH=3.

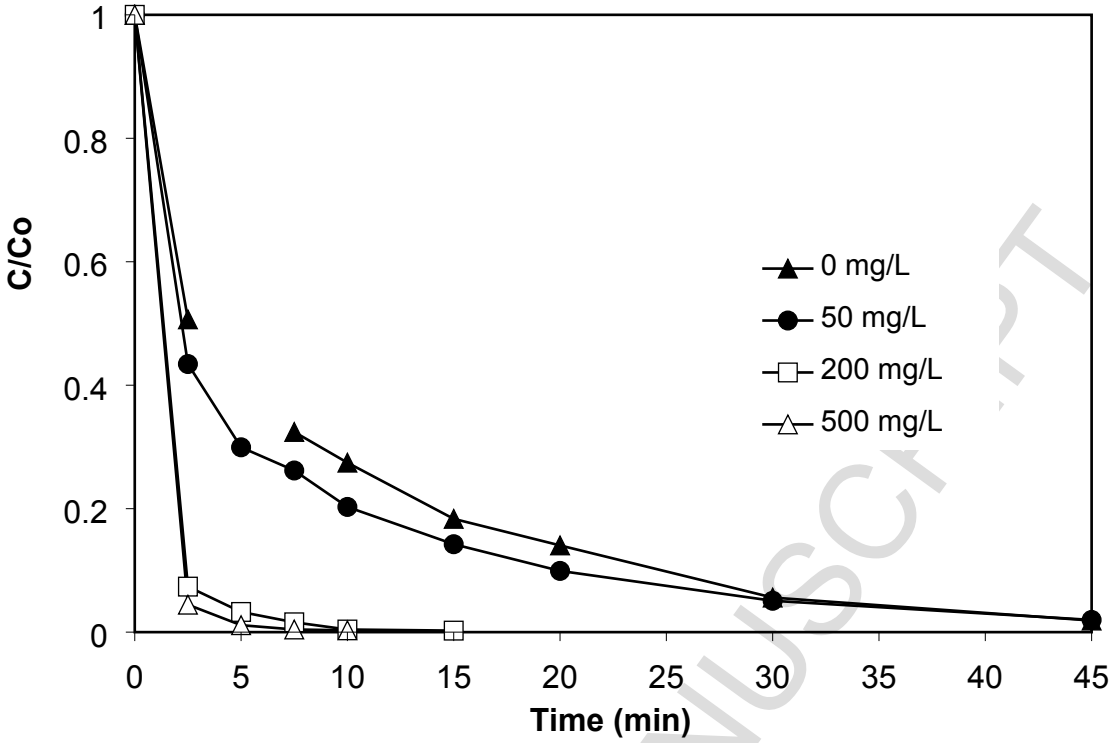

Figure 7. Effect of NaCl on 285 μg/L BPA degradation with 75 mg/L CX/CoFe and 250 mg/L SPS in UPW and pH=3.

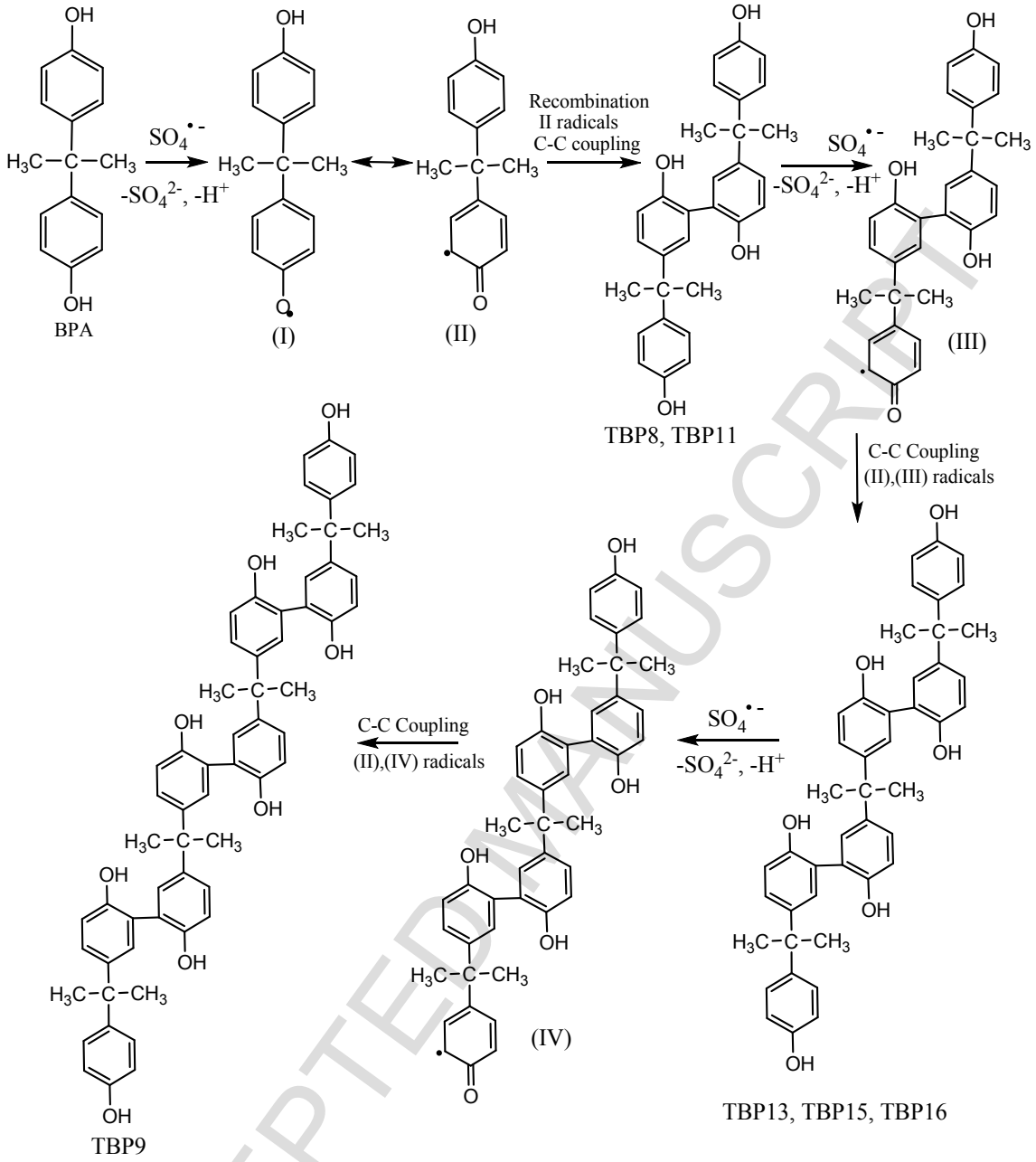

Figure 8. BPA transformation pathways by BPA-radical coupling during treatment with CX/CoFe and SPS in the presence and absence of NaCl.

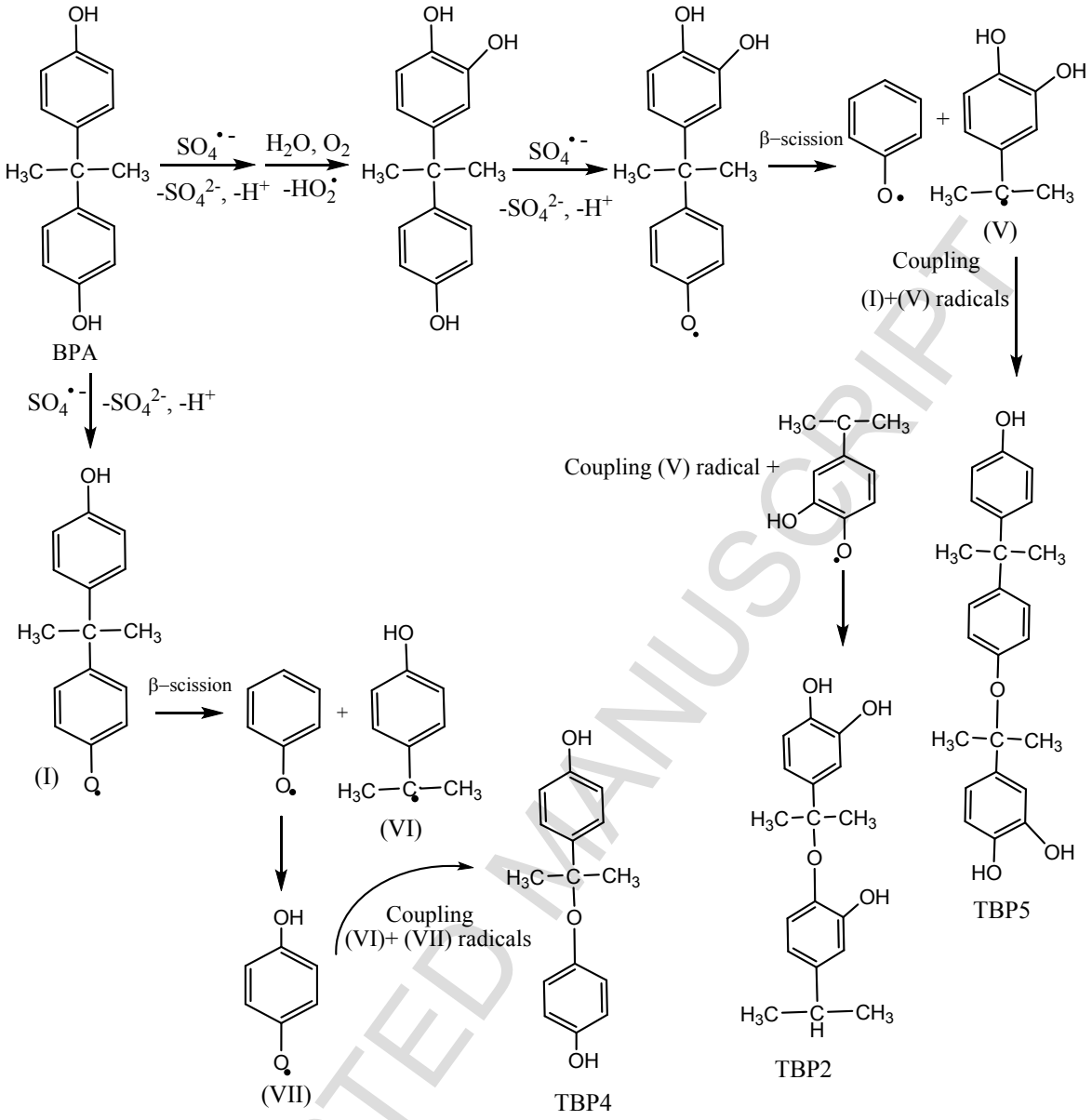

Figure 9. BPA transformation pathways by radical coupling after β-scission of BPA-radical during treatment with CX/CoFe and SPS in the presence and absence of NaCl.

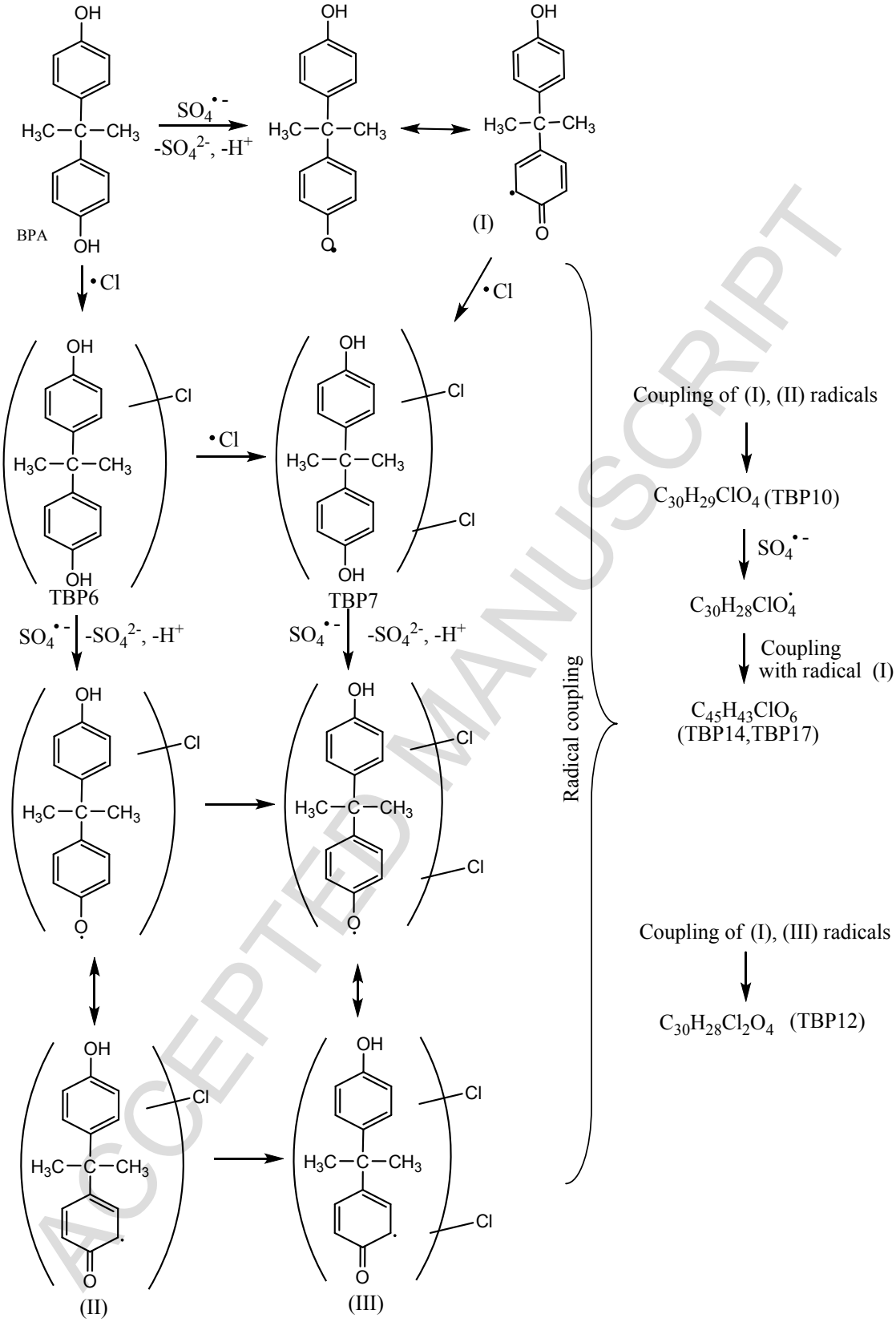

Figure 10. BPA transformation pathways during treatment with CX/CoFe and SPS in the presence of NaCl.

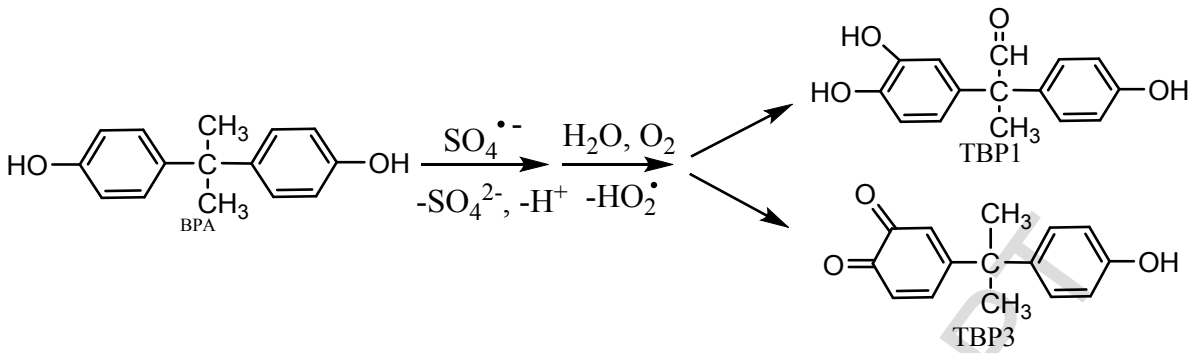

Figure 11. Hydroxylation degradation pathways of BPA during treatment with CX/CoFe and SPS in the absence of NaCl.

- Bimetallic Fe and Co carbon xerogels activate persulfate to sulfate radicals.
- BPA decomposition in environmental matrices is faster than in pure water.
- Chloride ion promotes degradation through the formation of chloride radicals.
- Catalyst/oxidant/substrate concentrations, pH and radical scavengers affect rates.
- Polymerization, bimolecular radical coupling and hydroxylation reactions dominate.

Table 1. Properties of the water matrices used in this work. ND: not determined.

Property	UPW	Wastewater	Drinking water	Surface water	Groundwater
pH	6	8	7.5	7.5	7.4
Conductivity, µS/cm	0.056	311	396	491	798
TOC, mg/L		7		2.7	1.9
Bicarbonate, mg/L		182	211	ND	ND
Chloride, mg/L		0.5	9.8	5	76
Sulfate, mg/L		30	15	274	69.5
Nitrate, mg/L		57	5		18.8

Table 2. High resolution accurate mass data ($[M-H]^-$, and relative error Δ(ppm)) for BPA and TBPs (a) in the absence of NaCl, and (b) in the presence of NaCl.

TBP code	Ion elemental composition	m/z $[M-H]^-$	Δ (ppm)	Process
BPA	$C_{15}H_{15}O_2$	227.1074	1.6	
TBP1	$C_{15}H_{13}O_4$	257.0821	-0.6	a
TBP2	$C_{18}H_{21}O_4$	301.1443	0.9	a
TBP3	$C_{15}H_{13}O_3$	241.0876	-2.4	a,b
TBP4	$C_{15}H_{15}O_3$	243.1028	-0.3	a,b
TBP5	$C_{24}H_{25}O_4$	377.1744	3.7	a,b
TBP6	$C_{15}H_{14}ClO_2$	261.0675	4.8	b
TBP7	$C_{15}H_{13}Cl_2O_2$	295.0297	0.4	b
TBP8	$C_{30}H_{29}O_4$	453.2059	2.8	a,b
TBP9	$C_{60}H_{57}O_8$	905.4019	4.4	a,b
TBP10	$C_{30}H_{28}ClO_4$	487.1682	-0.1	b
TBP11	$C_{30}H_{29}O_4$	453.2057	3.9	a,b
TBP12	$C_{30}H_{27}Cl_2O_4$	521.1280	2.4	b
TBP13	$C_{45}H_{43}O_6$	679.3059	0.8	a,b
TBP14	$C_{45}H_{42}ClO_6$	713.2649	3.7	b
TBP15	$C_{45}H_{43}O_6$	679.3041	3.6	a,b
TBP16	$C_{45}H_{43}O_6$	679.3065	0	a,b
TBP17	$C_{45}H_{42}ClO_6$	713.2675	0.1	b